ELSEVIER

NeuroImage

www.elsevier.com/locate/ynimg
NeuroImage 23 (2004) S97–S107

Surface-based approaches to spatial localization and registration in primate cerebral cortex

David C. Van Essen*

Department of Anatomy and Neurobiology, Washington University School of Medicine, St. Louis, MO 63110, United States

Available online 11 September 2004

Explicit surface reconstructions provide invaluable substrates for visualizing and analyzing the complex convolutions of cerebral cortex. This report illustrates the utility of surface-based atlases of human and macaque monkey for representing many aspects of cortical organization and function. These include a variety of cortical partitioning schemes plus an open-ended collection of complex activation patterns obtained from fMRI studies. Surface-based registration from one hemisphere to an atlas provides powerful approach to (i) objectively and quantitatively representing both the consistencies and the variability of the pattern of convolutions and the patterns of functional activation from any given task; and (ii) making comparisons across species and evaluating candidate homologies between cortical areas or functionally delineated regions.

Keywords: Cerebral cortex; fMRI; Cortical structure

Introduction

Structural and functional MRI have emerged as powerful techniques that can be routinely applied to humans and nonhuman primates. This has resulted in a vast outpouring of detailed information about the morphology and functional organization of primate cerebral cortex. To capitalize fully on this information, it is essential to have comparably powerful tools for visualizing and quantitatively analyzing complex spatial relationships relating to cortical structure and function. This entails dealing with a number of fundamental challenges. (i) The cortical sheet composes a complex mosaic of distinct areas (approximately 100 areas in macaque monkey and even more in human), each with its own specialized functions and internal organization (Van Essen, 2004a, in press; Jones and Peters, 1990a,b). (ii) The size of any given cortical area also shows marked variability (several fold) across individuals (Amunts et al., 2000; Rademacher et al., 2001; Van Essen et al., 1984). (iii) In many mammals, including humans and macaque monkeys, the cortex is a folded sheet of tissue whose convolutions allow a large surface area to fit compactly within the cranium. (iv) The pattern of convolutions shows marked variability across individuals, particularly in humans (Ono et al., 1990). (v) The location of any given cortical area is correlated with nearby geographic landmarks, but the strength of these correlations varies considerably across species and across regions within a species (Geyer et al., 1999; Lewis and Van Essen, 2000). Importantly, the last three points (species-specific convolutions, individual variability, and imperfect function–morphology correlations) are explicable in terms of a developmental mechanism (involving mechanical tension along long-distance corticocortical pathways) that is likely to underly cortical folding (Van Essen, 1997).

Over the past century, many methods have been developed to deal with cortical convolutions and their variability. Until recently, most efforts have involved volume-based approaches. These include the use of 3-D stereotaxic coordinate systems, volume- or slice-based atlases, and volumetric methods for registration of individual brains to an atlas (Thompson and Toga, 2002; Toga, 1999). However, volumetric and slice-based approaches have fundamental methodological limitations in relation to both visualization and registration. Fortunately, a powerful and complementary set of methods based on computerized cortical surface representations has emerged over the past decade (e.g., Drury et al., 1996, 1999; Fischl et al., 1999a,b; Schwartz et al., 1989; Van Essen et al., 2001, in press (a); Wandell et al., 2000). The keys to this approach involve (i) volume segmentations and explicit surface reconstructions that faithfully represent the shape of the cortical convolutions, including deep and irregular sulci; (ii) surface manipulations that facilitate visualization of complex geometry; (iii) surface-based atlases that provide a common spatial framework and a substrate for open-ended comparisons across data sets; and (iv) surface-based registration as a general way to compensate for individual shape differences and to facilitate interspecies comparisons. While acknowledging the complementarity of volume- and surface-based analyses, this article focuses on

* Department of Anatomy and Neurobiology, Washington University School of Medicine, 660 South Euclid Avenue, St. Louis, MO 63110. Fax: +1 314 747 3436.

Available online on ScienceDirect (www.sciencedirect.com.)

1053-8119/$ - see front matter © 2004 Elsevier Inc. All rights reserved.
doi:10.1016/j.neuroimage.2004.07.024

the surface-based approach, emphasizing recent progress using software tools developed in our laboratory (SureFit and Caret; http://brainmap.wustl.edu). One section illustrates surface representations for individual and atlas hemispheres of the macaque monkey and demonstrates how surface-based registration can be used to map data from individuals to the atlas. Another section illustrates surface representations for human cortex and demonstrates how the atlas can be used as a repository for both geographic information (e.g., probabilistic maps of cortical convolutions) and functional information (e.g., fMRI activation patterns from individuals and from population analyses). A third section illustrates how potential evolutionary relationships can be evaluated by registration between monkey and human cortical maps.

A key issue concerns what constitutes corresponding locations in any two hemispheres. Given the nature of the similarities and the differences between individual brains in their shapes and in functional organization, there cannot be any simple or single way to definitively establish precise correspondences throughout the cortex. A general need is for probabilistic representations that explicitly indicate different types of variability as well as experimental uncertainty and bias.

Another issue, introduced here and considered further in the Discussion section, is the growing need for electronic access to the tremendous amounts of information available about cortical structure and function. Traditional publication venues, even with online access, are inadequate to cope with this flood of data. However, recent developments with digital atlases and online databases offer exciting prospects for accelerating progress through new modes of communication and exploration.

Surface-based analyses of macaque cortex

Macaque individual and atlas surfaces

Fig. 1 illustrates surface reconstructions of the right hemisphere from two macaque monkeys, one chosen as an atlas (Case F99UA1, right panels) and another individual (Case M3) on the left. For both hemispheres, the SureFit method was used to generate surfaces running midway through the cortical thickness, thereby providing a balanced representation of gyral and sulcal regions (Van Essen et al., 2001). The figure shows lateral views of fiducial (3-D) surfaces (panels A and B), inflated surfaces (panels

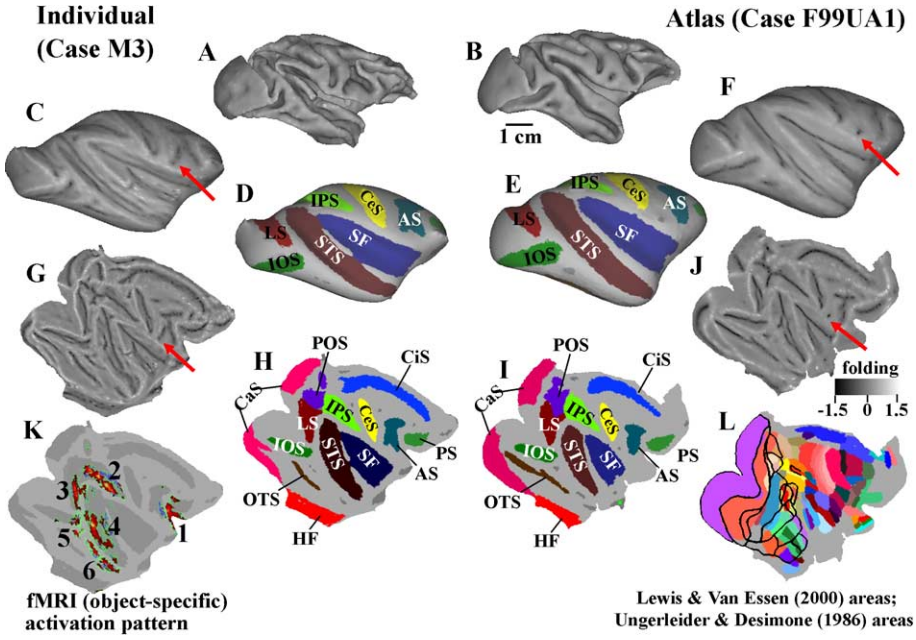

Fig. 1. Surface representations of individual and atlas macaque hemispheres in multiple configurations. (A and B) Lateral views of fiducial surface of an individual (case M3.R) and an atlas (F99UA1.R) right hemisphere. High resolution structural MRI of the individual brain (courtesy of G. Orban and K. Denys) and atlas brain (Rhesus monkey, courtesy of N. Logothetis) were segmented using the SureFit method. The atlas brain was selected on the basis of the high quality of the structural MRI data (0.5 mm voxel size) rather than on the basis of specific morphological characteristics. (C–F) Inflated maps of the individual and atlas surfaces, showing mean curvature (folding) and identified sulci. (G–J) Flat maps of the individual and atlas surfaces, again showing folding and identified sulci. The scale for folding (curvature) is in units of mm^{-1}, with negative corresponding to sulcal fundi and positive to gyral crowns. (K) fMRI activation pattern from viewing objects minus a scrambled objects control data from four individuals was registered to the Case M3 brain using a volume registration algorithm (Chefd'hotel et al., 2003) that achieved excellent alignment of the individual patterns (see Denys et al., 2004). Green regions surrounding the red/yellow activations reflect 0.5 mm spatial uncertainty in the alignment; blue represents activations that are likely to reflect spatial blur from a stronger focus in an opposing sulcal bank. (L) Architectonic areas and zones identified by Lewis and Van Essen (2000) in different colors, plus visual area boundaries identified by Ungerleider and Desimone (1986). Landmark-constrained registration of flat maps was used to align the data for each scheme (Van Essen, 2004a,b); see Fig. 3H for the probabilistic map from which the Lewis and Van Essen scheme was derived. Note: All data sets illustrated in this and subsequent figures can be accessed from the SumsDB database (http://brainmap.wustl.edu:8081/sums/directory.do?dirid=707162) for online visualization using WebCaret or for downloading and offline viewing and analysis using Caret. Abbreviations: AS = arcuate sulcus; CaS = calcarine sulcus; CeS = central sulcus; CiS = cingulate sulcus; HF = hippocampal fissure; IOS = inferior occipital sulcus; IPS = intraparietal sulcus; LS = lunate sulcus; POS = parietooccipital sulcus; PS = principal sulcus; OTS = occipitotemporal sulcus; SF = sylvian fissure; STS = superior temporal sulcus.

C–F) and flat maps (panels G–L). One set of inflated surfaces and flat maps (panels C, F, G, and J) displays a map of cortical folding (bright creases = gyral folds; creases = sulcal folds), thereby preserving detailed information about the original 3-D shape despite the differences in configuration. On another set (panels D, E, H, and I), 14 major sulci are shaded in distinct colors, revealing strong similarities in sulcal shape and location in each hemisphere. There are numerous differences in detail, however, including minor (secondary) folds or dimples that differ in size, location, or presence altogether (e.g., red arrows in panels C, F, G, and J). All of the modified surface representations inevitably have significant distortions relative to the fiducial surface. The flattening and spherical morphing algorithm used in Caret reduces areal and angular distortions based on an adjustable weighting of angular and linear forces (Drury et al., 1996). Several alternative strategies for distortion reduction have been developed, including minimization of an energy functional based on geodesic distances between nodes (Fischl et al., 1999a) and various strategies for achieving conformal (angle-preserving) mapping (Angenet et al., 1999; Gu and Yau, 2002; Ju et al., 2004).

Many types of experimental data can be displayed on individual and atlas cortical surface representations. Fig. 1K illustrates a functional MRI activation displayed on the individual hemisphere flat map. The fMRI pattern represents object-specific activations, based on the difference between viewing objects and scrambled versions of the same objects (Denys et al., 2004; the fMRI data from four monkeys, registered to case M3, see legend for details). As often occurs in fMRI studies, the spatial activation pattern is complex; here, it includes six major clusters over a large swath of extrastriate visual cortex (1–6 in Fig. 1K).

Fig. 1L illustrates a comparison between two cortical partitioning schemes displayed on the atlas map. This map uses various colors to represent the architectonic partitioning scheme of Lewis and Van Essen (2000) that covers most of the hemisphere, plus black outlines to indicate visual areas according to the Ungerleider and Desimone (1986) partitioning scheme. These two schemes, plus 10 other published schemes still in widespread use, have been mapped to the macaque atlas using surface-based registration (see below). Notably, the boundaries of most visual areas are not well correlated in the two schemes. Moreover, discrepancies of this sort are widespread when comparing any of the dozen partitioning schemes that have been mapped to the atlas (Van Essen, 2004a; Van Essen et al., in press (a)). This reflects the still rudimentary state of cortical cartography even in the most intensively studied nonhuman primate. Despite a remarkable century of progress, the field of cortical cartography is akin to the state of earth cartography centuries ago, when horses and sailing ships were the prime means for navigating the earth's surface!

Side-by-side comparison between the fMRI activations on the individual map (Fig. 1K) and partitioning schemes on the atlas map (Fig. 1L) naturally raises questions of which cortical area(s) are associated with each fMRI activation focus. However, it is inefficient and inaccurate to base such assessments on simple visual inspection, guided by nearby geographic landmarks. Instead, it is desirable to have objective methods for registering the entire individual map to the atlas surface.

Individual and atlas spherical maps

An initial step in facilitating surface-based comparisons is to map each hemisphere to a canonical shape and to define a corresponding surface-based coordinate system. Spherical maps have many advantages and are emerging as a standard for this purpose (Fischl et al., 1999a,b; Van Essen et al., 2001, in press (a)). Figs. 2B and C show spherical maps for an individual and an atlas hemisphere, respectively (same hemispheres as in Fig. 1). Each sphere was oriented to a standard spherical configuration after a process of minimizing distortions (see Fig. 2 legend). Lines of constant latitude and longitude are shown on each spherical map, and these have been projected to the flat maps in Figs. 2A and D.

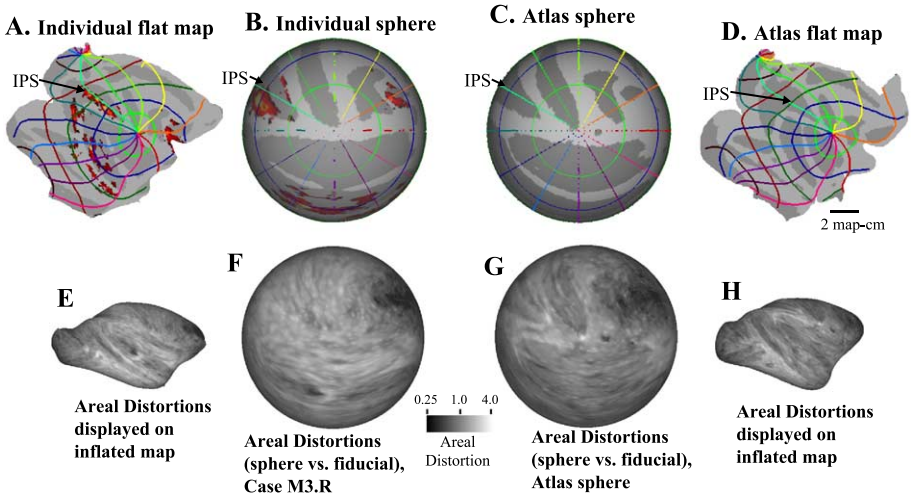

Fig. 2. Spherical maps and polar coordinate systems for the individual and atlas hemispheres. (A and B) Cartesian standard flat map and spherical standard map for Case M3.R, with lines of constant latitude and longitude generated on the sphere and projected to the flat map. To generate the flat map and spherical standard map, distortions relative to the fiducial surface were reduced using a multiresolution morphing algorithm (Drury et al., 1996) and the surfaces were then rotated and origins established according to established conventions (Drury et al., 1999). (C and D) Spherical standard map and cartesian standard flat map for the atlas hemisphere, processed in the same manner as the individual hemisphere. (E–H) Areal distortion for the spherical configuration relative to the fiducial configuration, displayed on inflated and spherical maps. Dark represents local compression of the spherical map and light represents local expansion. Other quantitative aspects of these distortions can be evaluated by downloading the data sets and visualizing and analyzing the distortions using Caret software.

Any given location can be specified by its coordinates, for example, latitude +28° and longitude −110° for the center of focus 4 in the STS.

A primary advantage of spherical coordinates is that they respect the topology (neighborhood relationships) of the cortical sheet, which is generally not the case for stereotaxic coordinates. However, because distortions cannot be completely eliminated when mapping the fiducial surface to a sphere, geodesic distances on the sphere are not identical to minimum intracortical distances. The residual distortions can be quantified using maps of areal distortion and linear distortion. Fig. 2 shows maps of areal distortion (ratio of fiducial to spherical map surface area) displayed on the spherical maps (panels F and G) and replicated on the inflated maps to facilitate orientation (panels E and H). These reveal a few regions of major compression (e.g., the frontal pole) or expansion (e.g., the juncture of temporal and frontal lobes), but relatively modest distortion over most regions (mostly less than twofold; note scale for panels E–G). The areal distortions are broadly similar in the two spherical maps but differ in their details.

After each hemisphere has been rotated to a standard spherical configuration, corresponding geographical structures (e.g., IPS, the intraparietal sulcus) on the individual and atlas spherical standard maps have similar but not identical locations (Figs. 2B and C). The differences reflect the intrinsic variability in 3-D shape combined with the variable patterns of distortion when mapping to a sphere. To improve the alignment between spheres from different individuals requires a higher dimensional (nonrigid) transformation. However, if the class of deformations is restricted to topology-preserving spherical deformations, the registration problem is greatly simplified relative to the challenges of respecting cortical topology using volume-based registration.

Surface-based registration

The objective of within-species registration is to map each location in one hemisphere to the 'corresponding' location in another hemisphere (an atlas or another individual). But what constitutes correspondence, given the imperfect correlation between functional subdivisions and nearby morphological features in each hemisphere? If the objective is to align functionally corresponding regions as precisely as possible, then it would be desirable to invoke functional and/or architectonic data as primary constraints in the registration process. However, in most situations, reliable functional landmarks are not consistently available or adequate; consequently, it is generally necessary to rely on geographic information as the primary or exclusive substrate for registration between individuals. For registration across species, the situation is different [see 'Interspecies (Monkey–human) comparisons section'].

For the macaque, the dependence on geographic landmarks is not a severe problem because (i) the major sulci and gyri are consistently present and are readily identifiable on surface reconstructions (cf. Fig. 1), and (ii) cortical areas have a reasonably consistent location relative to major geographic landmarks in the macaque. The variability in areal boundaries relative to gyral or sulcal creases is typically 1–3 mm (Lewis and Van Essen, 2000; see Fig. 3H below).

Several methods have been developed for surface-based registration. They differ in how the constraints on registration are specified, the algorithms used to reduce unwanted local distortions, and the geometry of the surface representation. One general approach involves constraining the registration process using explicitly defined landmark contours (Glaunes et al., 2004; Van Essen et al., 1998, 2001, in press (a); Thompson et al., 2000, 2003). An alternative approach is to constrain the registration using continuously varying shape metrics such as cortical convexity (Fischl et al., 1999a,b). The distortion-reducing algorithms include fluid deformation (Joshi et al., 1997); minimization of an energy functional involving average convexity and metric distortion (Fischl et al., 1999a,b); elastic warping (Thompson and Toga, 2002; Thompson et al., 2000); and iterative application of landmark-constrained smoothing and shape-preserving forces (Van Essen et al., in press (a)). Regarding surface geometry, registration algorithms may operate on spherical maps for the entire hemisphere (Fischl et al., 1999b; Van Essen et al., 2001), flat maps of part or all of the hemisphere (Van Essen et al., 1998, in press (a)), and spherical or flat map representations of the external hull of the hemisphere that lack an explicit representation of buried cortex (Thompson et al., 2000, 2003). There are important trade-offs between these various methods on both theoretical and practical grounds. It is an empirical issue how well each method succeeds in reducing individual variability for actual data sets (see Discussion section). In the example illustrated in Fig. 3, a set of 15 corresponding landmarks were drawn on the individual and atlas flat maps, running along the fundi of major sulci (Figs. 3A and C). These landmarks (plus a cartesian grid on the individual flat map) were projected to the corresponding spherical maps (Figs. 3D and F), where the landmark-constrained registration algorithm was applied. The deformed cartesian grid and individual folding map, displayed on the atlas sphere (Fig. 3E) and atlas flat map (Fig. 3B), indicate that relatively moderate deformations (mostly less than twofold in surface area) were needed to obtain good registration. Fig. 3G provides another illustration of the difference between individual and atlas spherical maps, by comparing latitude and longitude isocontours determined for the atlas sphere (thin contours) to the corresponding isocontours deformed from the individual to the atlas (thick contours). The differences are everywhere modest: A given polar coordinate represents slightly different geographic locations on individual and atlas maps; conversely, a given geographic location has modestly different polar coordinates for the individual and atlas. For example, the center of fMRI activation focus 4, whose coordinates were (+28°, −110°) on the individual map, has coordinates (+20°, −117°) after registration to the atlas. Both sets of spherical coordinates (individual and atlas) can be appropriate to invoke under one or another analysis situation, but the example also highlights the importance of including the reference frame used when stating coordinates.

Given the known variability in size and location of each cortical area, it is desirable to represent this variability in a probabilistic manner. Fig. 3H shows a probabilistic architectonic map for the Lewis and Van Essen (2000) scheme based on data from five individual hemispheres registered to the atlas. The likelihood that each atlas location is associated with one or another area is represented by the saturation level for each hue, with maximal saturation indicating locations consistently associated with a particular cortical area. Regions of lower consistency reflect the aggregate effects of individual variability in areal size, experimental uncertainties in charting subtle architectonic boundaries, and methodological factors that affect the deformation from individual maps to the atlas. Overlaid on this probabilistic map

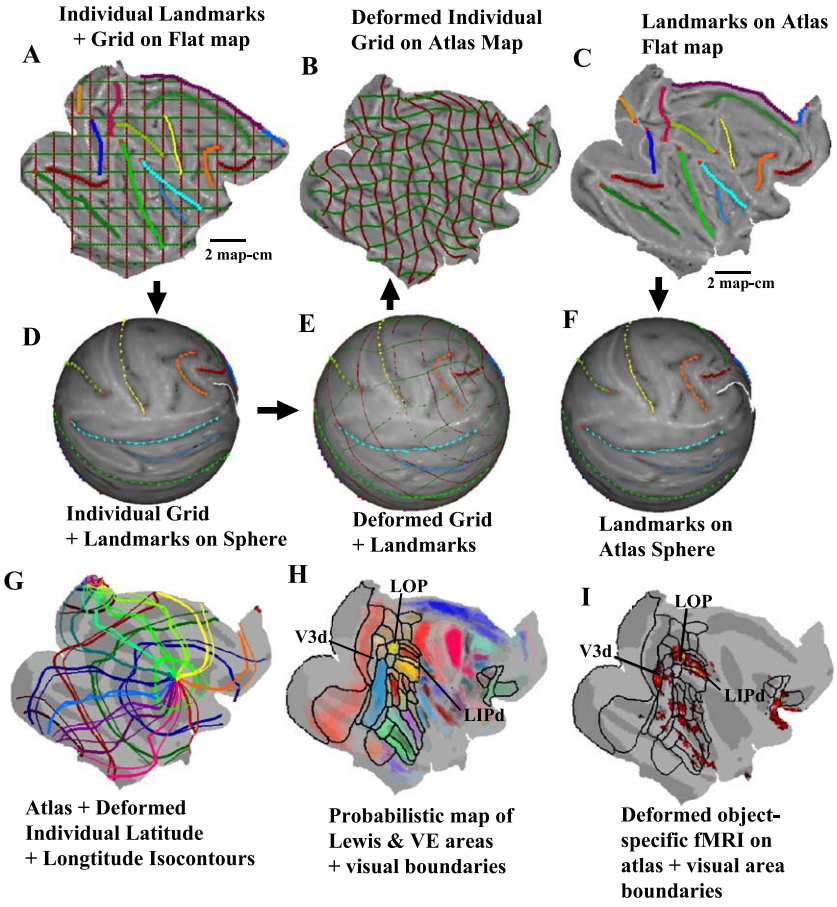

Fig. 3. Surface-based registration between individual and atlas maps. (A) Landmarks (sulcal fundi and hemispheric margins) plus cartesian grid lines on the individual flat map. (D) Landmarks and grid projected to individual spherical map. (C) Corresponding landmarks on the atlas flat map. (F) Landmarks projected to the atlas spherical map. (E) Deformed landmarks and grid displayed on the atlas spherical map. (B) Deformed landmarks and grid on the atlas flat map. The registration between individual and atlas spherical maps was achieved by a multicycle process that initially forces corresponding landmark points into register and reduces distortions of intervening regions by a combination of landmark-constrained smoothing and shape-preserving morphing forces (Drury et al., 1996; Van Essen et al., 2001). (G) Atlas latitude and longitude isopolar contours (same as Figs. 2C and D) plus deformed latitude and longitude isopolar contours registered from the individual (same as Figs. 2A and B) to the atlas map. (H) Probabilistic map of Lewis and Van Essen (2000) architectonic areas from five individual hemispheres registered to the atlas (Van Essen et al., in press (a)), plus areal boundary contours indicating the most likely location of each boundary. (I) Deformed object-specific fMRI activation pattern registered from the individual map (Fig. 1K) to the atlas map and overlaid by the Lewis and Van Essen boundaries.

are the estimated locations for the most likely boundary of each visual area. Several visual areas or zones relevant to the comparison with object-specific fMRI activations are identified in this panel (V3d, LIPd, LOP); other areas can be identified using online or offline visualization options available for these data sets (see Fig. 3 legend and discussion). The visual area boundaries are replicated in Fig. 3I and are overlaid on the fMRI activation pattern from case M3.R registered to the atlas. This overlay allows detailed assessments, such as the observation that focus 3 is centered in V3d; focus 2 is strongest in LIPd but also extends into neighboring areas LIPv and LOP.

Human surface-based analyses

Human individual and atlas maps

Human cerebral cortex, with its 10-fold greater surface area than that of the macaque, is far more convoluted and also much more variable across individuals (Ono et al., 1990). This is illustrated in Fig. 4 using surface reconstructions of the right hemispheres of an atlas brain (‘colin,’ bottom row) and another normal brain (Buckner—Case 1, top row). In both cases, the surface reconstruction faithfully reflects the full complexity of cortical convolutions, including minor wrinkles and dimples, as revealed by scrolling through the structural MRI volume with the volume segmentation overlaid (http://brainmap.wustl.edu:8081/sums/directory.do?dirid=707144). Importantly, the quality of surface reconstructions generated using available segmentation tools varies widely not infrequently, the surfaces fail to capture many of the major cortical sulci (e.g., Angenet et al., 1999).

In Figs. 4A–F, about two dozen sulci have been identified in each hemisphere, as indicated by different hues and by explicit labels on a subset of sulci. In contrast to the relatively consistent size, shape, and position of identifiable sulci in the macaque, prominent differences between correspondingly named human sulci are evident in the fiducial, inflated, and flat map configurations (Figs. 4A–C vs. D–F). For example, the lateral occipital sulcus

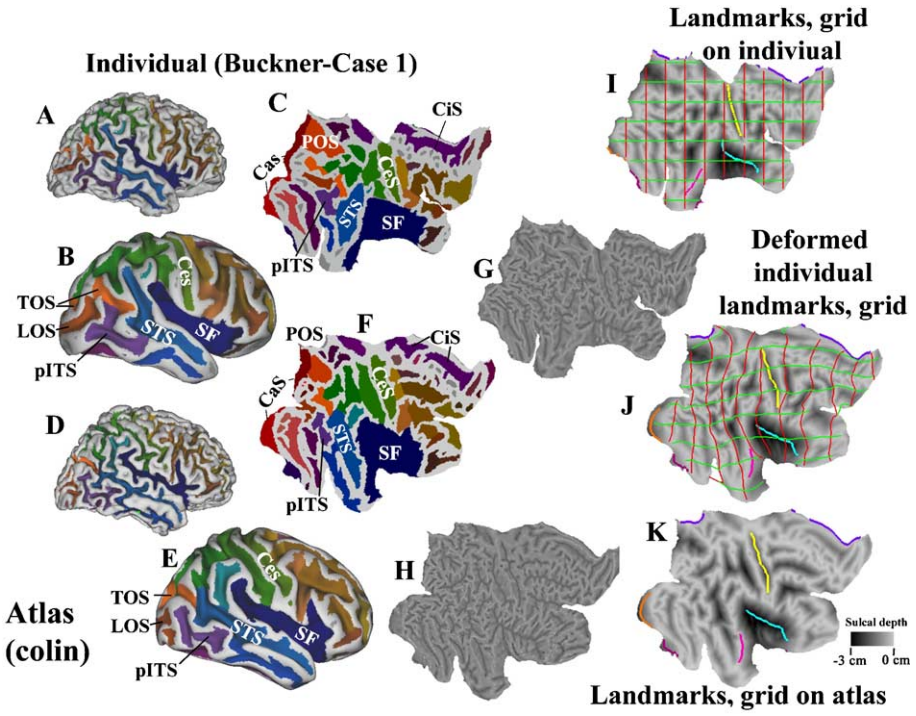

Fig. 4. Surface representations of individual and atlas human right hemispheres. (A–C) Fiducial, inflated, and flat map surfaces of individual hemisphere (Case 1, structural MRI data set courtesy of R. Buckner), with individual sulci shaded in different hues and selected sulci labeled. (D–F) Fiducial, inflated, and flat map surfaces of atlas hemisphere ('colin,' structural MRI data set courtesy of A. Toga, C. Holmes; Holmes et al., 1998), with individual sulci shaded and labeled. Abbreviations as in text and Fig. 1 legend. (G and H) Flat maps of individual and atlas hemispheres shaded to indicate cortical folding, thereby revealing shape characteristics in finer detail. (I) Registration landmarks and cartesian grid on individual flat map, overlaid on map of cortical depth determined from the fiducial configuration (darker is deeper). (K) Registration landmarks for atlas flat map, overlaid on a map of cortical depth. (J) Deformed grid and landmarks from registering the individual to the atlas via spherical surface-based registration. Landmarks include the fundi of the central, Sylvian, and calcarine sulci, the anterior superior temporal gyrus, and the dorsal and ventral margins of medial wall cortex.

(LOS), transverse occipital sulcus (TOS), and posterior inferior temporal sulcus (pITS) are each identifiable in both hemispheres, but they differ markedly in size, shape, and exact location. Maps of cortical folding (Figs. 4G and H) provide an even more detailed representation of shape, as illustrated already for the macaque.

Besides the greater variability in the pattern of convolutions, the relationship of various cortical areas to sulcal and gyral boundaries is also more variable in humans than in the macaque. The consistencies appear to be somewhat better for primary sensory areas, including V1 relative to the calcarine sulcus (Amunts et al., 2000), somatosensory cortex relative to the central sulcus (Geyer et al., 1999), and auditory cortex relative to Heschl's gyrus (Rademacher et al., 2001) than for higher areas (Angenet et al., 1999; Amunts et al., 2004; Grefkes et al., 2001). Outside the primary areas, the variability is large enough to make it debatable whether additional geographic landmarks provide a net help or a net hindrance in constraining registration between hemispheres. This cannot be resolved on theoretical grounds but instead needs to be evaluated by carefully conducted empirical analyses that have yet to be conducted. Landmark-based spherical surface registration is particularly well suited for such analyses because it readily allows selective application of geographic constraints, and the effects of adding or removing landmarks can be assessed objectively. Fischl et al. (1999b) use an alternate strategy in which the degree to which shape characteristics (convexity) constrain the registration is regulated by the variability at each location. In contrast, volume-based registration strategies that selectively emphasize particular geographic landmarks or characteristics, while also respecting cortical topology, would be vastly more complex to design and implement.

Figs. 4I–K illustrates the deformation of Case 1 to the atlas using landmark-constrained spherical registration. A set of six corresponding landmarks for Case 1 (panel I) and the atlas (panel K) are overlaid on maps of sulcal depth (darker corresponds to deeper; depth is computed as the distance from a 'cerebral hull' surface that runs along the external margins of the hemisphere without diving into sulci). This provides a useful representation of cortical shape that differs from the maps of folding and of buried cortex used in adjacent panels. Registration between the individual and atlas was carried out on spherical maps (not illustrated); the deformed cartesian grid and the deformed sulcal depth map from Case 1 are shown on the atlas flat map in panel J. In general, the deformed cartesian grid shows only modest regional variations, and the degree of differential expansion or shearing needed to achieve registration was nowhere severe (90% of the surface was deformed less than twofold, based on surface areas for corresponding locations in the fiducial surfaces).

Probabilistic maps of sulcal depth

This registration strategy was applied to a total of six normal right hemispheres, and the resultant deformed sulcal depth maps for these individuals are shown in Figs. 5B–G, along with the sulcal depth map for the atlas hemisphere (Fig. 5A). The consistencies as well as differences across individuals are much easier to visualize by having sulcal depth patterns represented on

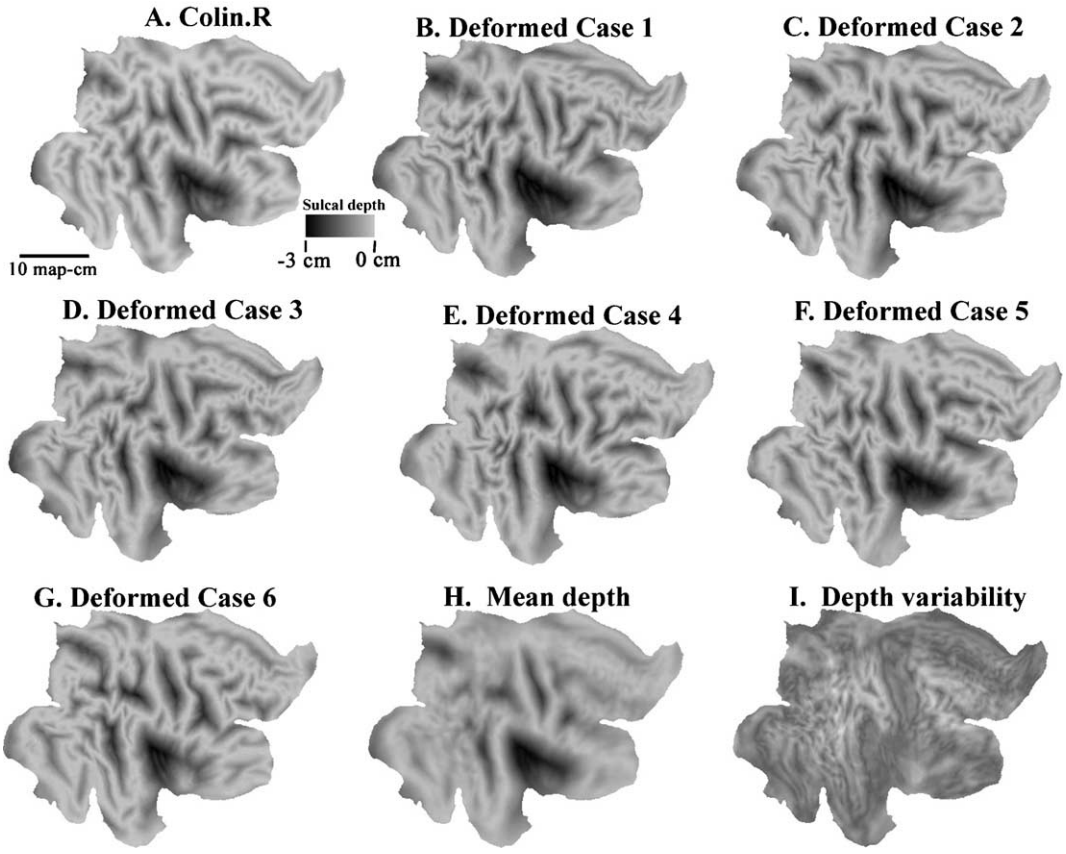

Fig. 5. Surface depth maps from individuals registered to atlas maps. (A) Cortical depth map for the atlas surface. (B–G) Deformed cortical depth maps for Buckner Cases 1–6, registered to the atlas as indicated in Figs. 4I–K. (H) Mean depth map, obtained by computing the mean across maps A–G at each location. (I) Depth variability map, indicating the standard deviation for the mean depth map, with darker shades indicating smaller standard deviation (lower variability) and lighter shades indicating larger standard deviation (higher variability).

the common framework provided by the atlas flat map. This also allows objective, quantitative analyses of shape characteristics to be carried out, as exemplified by the map of mean sulcal depth (panel H) computed across all seven depth maps. The 'depth variability' map in Fig. 5I was generated by computing the standard deviation of the mean depth, then spatially smoothing to reduce minor local fluctuations. Regions of low depth variability are indicated in dark shades and regions of high variability in light shades. The least variable regions include the central and calcarine sulci (and their adjoining gyral banks), the Sylvian fissure, part of the STS, and the dorsomedial convexity (DMC) in prefrontal cortex. Regions of high depth variability include portions of parietal cortex and dorsolateral prefrontal cortex. These maps of mean depth and its variability provide a probabilistic representation in which surface shape attributes at each point on the map reflect the properties of the population rather than any individual, including the atlas surface that is the target of registration. The availability of probabilistic maps can help alleviates concern about the use of one particular hemisphere as the spatial coordinate system for a surface-based cortical atlas (see Discussion section).

Mapping functional data onto the human atlas

As noted in the Introduction, most human functional imaging studies have used volume-based registration strategies to compare results across individuals. In principle, though, surface-based registration should be more effective at reducing intersubject variability (Drury et al., 1999; Fischl et al., 1999b). Fig. 6 shows a direct comparison of these two approaches using data obtained using a paradigm in which subjects viewed images of objects and scrambled objects (Denys et al., 2004), in a paradigm identical to that used for the monkey fMRI results in Figs. 1–3, Fig. 6A–F shows results for two individual subjects, where data were mapped onto surface reconstructions and flat maps. In this study, the surface reconstructions were initially generated using FreeSurfer software (http://surfer.nmr.mgh.harvard.edu), which generates surfaces that run along the gray or white matter border and have sharp creases along gyral ridges, thus yielding a different appearance compared to the SureFit-generated surfaces and maps of folding in Figs. 4 and 5. In both subjects, activations are concentrated in the lateral occipital (LO) complex near the occipitotemporal junction but also extend into portions of dorsal–occipital and parietal cortex. The two individual hemispheres were registered to the atlas surface using landmark-based spherical registration; the resultant activations after deformation to the atlas are shown in panels G and H, where they can be more readily compared with one another and with other data such as the location of topographically organized visual areas that have been mapped to the atlas. The main activations are centered at latitude -26°, -136° longitude, between area V8 below and areas MT+ and LOS (the lateral occipital sulcus region, a.k.a. LOC/LOP) above. There are some

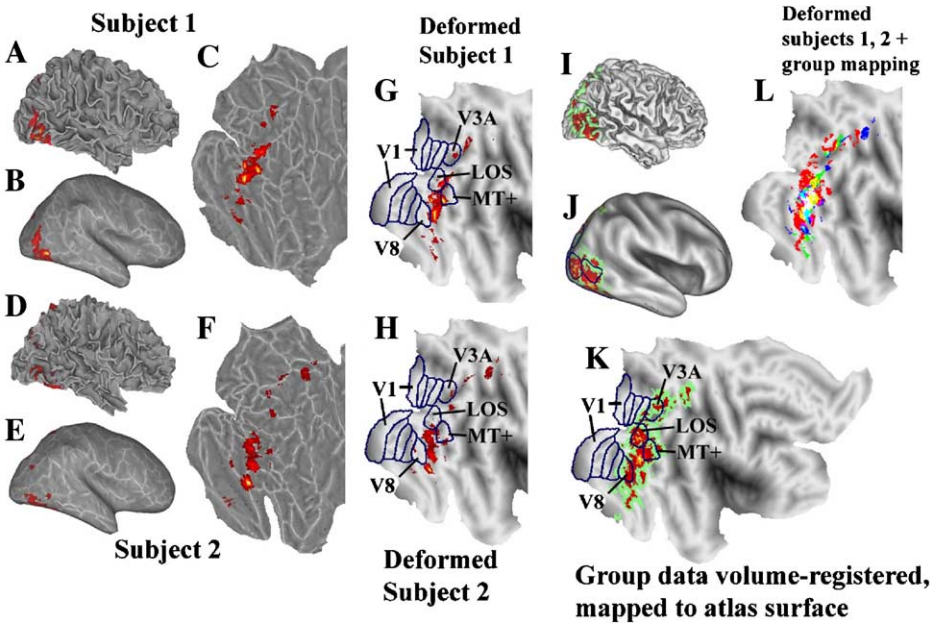

Fig. 6. Comparison of surface- and volume-based mapping of human fMRI data onto atlases. (A–C) Object-specific fMRI activation pattern in Subject 1 from Denys et al. (2004). Surface reconstructions were generated using FreeSurfer software, but the maps were converted to Caret format to facilitate comparisons and to allow registration to the atlas surface. Flat map (only posterior cortex shown) was generated using Caret. (D–F) Object-specific fMRI activation in Subject 2. (G and H) Deformed fMRI activations from Subjects 1 and 2 registered to the atlas. (I–K) Group-average fMRI for 17 subjects using the same paradigm registered to stereotaxic space in SPM and tested by a random effects analysis to insure generality of the results. Red and yellow represent significant activations; green represents surface locations within 3 mm of these activations, thereby reflecting the spatial uncertainties associated with population-averaged volume data. (L) Comparison across object-specific activations from deformed Subject 1 (green), deformed Subject 2 (blue), and group-activation (red). Yellow, purple, and white represent regions of overlap of the three primary patterns. (For interpretation of the references to colour in this figure legend, the reader is referred to the web version of this article.)

differences in detail, particularly in the parietal lobe activations in the two individuals. In the volume-based analysis for this study, fMRI data from 17 subjects were aligned to a common stereotaxic space by nonlinear volumetric registration (SPM; Friston et al., 1995), and the results were mapped to the colin right hemisphere atlas (Figs. 6I–K). (The green halos surrounding the red/yellow group activation data are an indication of the approximate spatial uncertainty associated with volume-based registration.) The group activation occupies a larger extent of the atlas, including a larger portion of MT+, V8, and LOS than in either the Subject 1 or 2 maps. Additional differences across patterns are illustrated in panel L, which overlays the pattern for Subject 1 (green), Subject 2 (blue), and the group activation (red). A key issue raised by this initial comparison is whether the greater apparent spread for the volume-based analysis reflects increased sensitivity from the larger number of subjects, increased spatial spread because of limitations of volume-based registration, or a combination of these factors. Systematic comparisons in which volume- and surface-based registration are applied to the same data sets for a large population are essential in order to resolve this issue in general and to evaluate different strategies for surface-based registration.

Interspecies (Monkey–human) comparisons

The results illustrated here for the macaque (Figs. 1–3) and human (Figs. 4–6) naturally invite detailed comparisons of cortical organization across species. The macaque is the most intensively studied nonhuman primate for studies of cerebral cortex, making it especially important to understand both the commonalities and the species differences in functional organization. This is inherently challenging owing to the dramatic differences in the complexity of convolutions. The problem is compounded by the fact that geographic landmarks can be unreliable insofar as homologous areas in the two species (e.g., area V1) can have markedly different locations in relation to sulcal landmarks such as the calcarine sulcus. Both of these problems can be readily addressed using landmark-based registration of spherical maps. One spherical map can be registered to another constrained by any desired combination of functional and geographic landmarks, while avoiding interference from geographical landmarks that do not provide useful constraints.

This approach has been used in several recent studies to explore the implications associated with various proposed homologies (Astafiev et al., 2003; Denys et al., 2004; Van Essen, 2004a, in press; Van Essen et al., in press (a)). For example, a standard set of 10 landmarks has been identified, based on presumed homologies for visual areas V1, V2, MT, and the frontal eye fields; primary auditory, olfactory or gustatory, and somatosensory or motor areas; and corresponding regions along the medial wall of the hemisphere (Van Essen, 2004a, in press). A deformation from macaque to human cortex based on these landmarks results in a large expansion of parietal, temporal, and frontal cortex, but much less expansion of occipital cortex. When this deformation was applied to the monkey object-sensitive fMRI activations (Fig. 1K and 7A), the deformed macaque fMRI activation (green in Fig. 7C) showed relatively little overlap (yellow) with the human object-sensitive activations in temporal and parietal cortex (Figs. 6K, 7B, and red in 7C). On the one hand, this mismatch might signify a

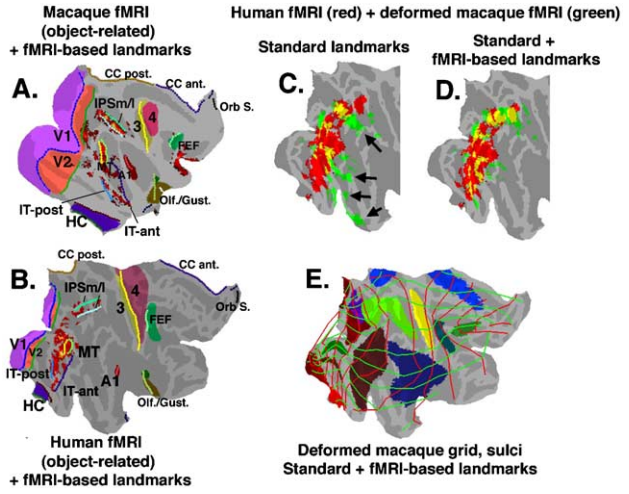

Fig. 7. Surface-based registration between macaque and human cortex. (A) Standard plus fMRI-based landmarks on the macaque flat map. (B) Corresponding standard plus fMRI-based landmarks on the human flat map. (C) Object-specific fMRI activations for human (red) an deformed macaque (green) based on registration using standard landmarks. (D) Object-specific activations for human (red) and deformed macaque (green) based on standard plus fMRI-based landmarks. Yellow in panels (C and D) indicates overlap. (E) Deformed cartesian grid and deformed macaque sulci (colors as in Fig. 1) based on standard plus fMRI-based landmarks.

major species difference in the functional organization of object-processing cortical areas. However, an attractive alternative is that the activation patterns do indeed correspond to homologous regions. This hypothesis can be explored by including the fMRI activation patterns in parietal and temporal cortex as additional constraints on interspecies registration (landmarks IPS/m/l, IT-post, IT-ant in Figs. 7A and B), thereby yielding much greater overlap of the human and deformed macaque object-sensitive activations (yellow in Fig. 7D). The resultant registration, shown in Fig. 7E with deformed macaque sulci plus a deformed cartesian grid, suggests a preferential expansion of lateral parietal and dorsoanterior temporal cortex, perhaps indicative of a domain where new areas emerged in humans or existing ones expanded very nonuniformly in the two species. Note that this registration involves a highly nonuniform deformation of the macaque intraparietal sulcus (green), including regions that have been hypothesized on other grounds to have undergone rapid evolution in the human lineage (Simon et al., 2002; Orban et al., 2004). While this general approach cannot prove or disprove any particular hypothesized homology, it does provide a sound and objective basis for exploring complex patterns of hypothesized homologies and their implications for the relationships among nearby areas in the two species.

Discussion

In the early years of computerized brain mapping during the preceding decade, progress using surface-based analyses of cerebral cortex was hampered by a combination of methodological limitations (surfaces were difficult to generate and manipulate using software available at the time) and widespread skepticism about the need for or utility of surface-based approaches. While neither set of obstacles has vanished, currently available software tools are vastly more powerful and user-friendly, and the number of publications making use of surface-based analyses has grown dramatically. Issues that are important to discuss in the context of this article include the evolving role and intertwined nature of surface-based atlases, probabilistic atlases, surface-based coordinates, and surface-based registration.

Atlases, coordinate systems, and probabilistic representations

Modern brain atlases have much to offer (Thompson and Toga, 2002; Van Essen, 2002): (i) a common spatial framework that compensates for some but not all aspects of individual variability; (ii) visualization substrates for viewing a variety of brain structures and spatial relationships among them; (iii) spatial coordinate systems that allow concise and objective descriptions of precise locations in atlases and individuals; (iv) probabilistic representations reflecting aspects of individual variability that cannot be compensated by existing spatial normalization methods; and (v) online availability to facilitate widespread access and utilization.

Selection of any particular brain as an atlas poses the obvious risk that the shape characteristics of the individual may introduce unwanted biases in subsequent analyses carried out using the corresponding atlas space. This has been an acute issue in the context of Talairach stereotaxic space for volume representations because the Talairach and Tournoux (1988) brain differs markedly from the average brain dimensions in a population of normal adults. One strategy for addressing this problem is to average the intensity values of structural MRI volumes from a population of subjects after registration to the original Talairach space (Ojemann et al., 1997), or after registering brains to a target that matches the average dimensions of the population (Evans et al., 1994; Friston et al., 1995). The ‘fuzziness’ of the associated population-average MRI volumes varies, reflecting the degree to which the registration algorithm has reduced shape variability. Because several versions of stereotaxic space and many registration algorithms are in common use in human neuroimaging studies, a given location in an individual brain can have markedly different coordinates according to the choice of stereotaxic space and registration.

The surface-based population shape maps illustrated here (Fig. 5) are analogous in some ways to a population-average structural MRI, but they offer significant advantages. In essence, each location on an atlas sphere can be associated with multiple shape characteristics (e.g., cortical folding as well as depth) and also geographic characteristics (sulcal and gyral identity) with each characteristic reflecting statistical properties derived from a population of individuals. Displaying these characteristics on flat maps of the atlas surface is convenient for visualizing the entire surface in a single view, but the key relationships reflect statistical attributes computed on the spherical map. Moreover, quantitative analyses, such as surface areas of various regions of interests (e.g., a particular sulcus), can be based on actual values in the individual fiducial hemispheres even if these regions are identified after deformation to the atlas map. An attractive alternative is to generate probabilistic maps by registering individual hemispheres to an atlas sphere whose landmarks represent shape characteristics of many individuals (D.C. Van Essen, unpublished data). By either of these approaches or by alternative surface-based population-averaging algorithms (e.g., Fischl et al., 1999b), a growing arsenal of normal population

shape maps will in turn provide an invaluable baseline for making comparisons with potential shape abnormalities in populations of subjects associated with a variety of neurological or psychiatric diseases (Kuperberg et al., 2003; Rosas et al., 2002; Van Essen et al., in press(b)).

Databases and online visualization

In order to make best use of the torrents of digital neuroimaging data emerging from laboratories around the world, it is increasingly important to have rapid and flexible access to these data. The surface-based atlases and visualization methods discussed in this article provide important components of the infrastructure needed for this purpose. Another key component involves databases that provide centralized repositories for neuroimaging data. The fMRI Data Center (Van Horn et al., 2001; http://fmridc.org) is one such repository that is customized for volume-related fMRI data. Our laboratory has developed a complementary database SumsDB (http://brainmap.wustl.edu:8081/sums) that is a repository mainly for surface-related data but able to handle volume data as well (Dickson et al., 2001; Van Essen et al., in press (a)). SumsDB provides access to other data not just for macaque and human cerebral cortex as illustrated here, but also for cerebellar cortex and for rodent (mouse and rat) atlases, and it includes many individual data sets as well as the atlases. These data sets can be downloaded for offline analysis using Caret, but they are also accessible for online visualization using WebCaret. As an illustration, all of the data in Figs. 1–6 are accessible via SumsDB from a single hyperlink (http://brainmap.wustl.edu:8081/sums/directory.do?dirid=707162), which links to a SumsDB directory containing the individual specification files and associated data sets. Users can simply click on the relevant 'Visualize' option to view the corresponding surface representation online.

In summary, the turn of the century has coincided with rapid advances in many facets of acquiring, analyzing, communicating, and interpreting neuroimaging-related data. These advances hold tremendous promise for better understanding of the function of cerebral cortex in health and disease.

Acknowledgments

I thank J. Harwell, D. Hanlon, and J. Dickson for invaluable efforts in software development, E. Reid for data analysis, S. Danker for manuscript preparation, and G. Orban, K. Denys, W. Vanduffel, and R. Buckner for providing access to their published data sets via SumsDB. Supported by a Human Brain Project/Neuroinformatics research grant funded jointly by the National Institute of Mental Health, National Science Foundation, National Cancer Institute, National Library of Medicine and the National Aeronautics and Space Administration (R01 MH60974-06), and The National Partnership for Advanced Computational Infrastructure (NPACI).

References

Amunts, K., Malikovic, A., Mohlberg, H., Schormann, T., Zilles, K., 2000. Brodmann's areas 17 and 18 brought into stereotaxic space—where and how variable? NeuroImage 11, 66–84.

Amunts, K., Weiss, P.H., Mohlberg, H., Pieperhoff, P., Eickhoff, S., Gurd, J.M., Marshall, J.C., Shah, N.J., Fing, G.R., Zilles, K., 2004. Analysis of neural mechanisms underlying verbal fluency in cytoarchitectonically defined stereotaxic space—The roles of Brodmann areas 44 and 45. NeuroImage 22, 42–56.

Angenet, S., Haker, S., Tannenbaum, A., Kikinis, R., 1999. On the Laplace–Beltrami operator and brain surface flattening. IEEE Trans. Med. Imag. 18, 700–7119.

Astafiev, S.V., Shulman, G.L., Stanley, C.M., Snyder, A.Z., Van Essen, D.C., Corbetta, M., 2003. Functional organization of human intraparietal and frontal cortex for attending, looking, and pointing. J. Neurosci. 23, 4689–4699.

Chefd'hotel, C., Hermosillo, G., Faugeras, O., 2003. Flows of diffeomorphisms for multimodal image registration. Proc. IEEE Int. Symp. Biomed. Imag. 7–8, 753–756.

Denys, K., Vanduffel, W., Fize, D., Nelissen, K., Peuskens, H., Van Essen, D., Orban, G.A., 2004. The processing of visual shape in the cerebral cortex of human and non-human primates: a functional magnetic resonance imaging study. J. Neurosci. 24, 2551–2565.

Dickson, J., Drury, H., Van Essen, D.C., 2001. The surface management system (SuMS) database: A surface-based database to aid cortical surface reconstruction, visualization and analysis. Philos. Trans. R. Soc. Ser. B 356, 1277–1292.

Drury, H.A., Van Essen, D.C., Anderson, C.H., Lee, C.W., Coogan, T.A., Lewis, J.W., 1996. Computerized mappings of the cerebral cortex. A multiresolution flattening method and a surface-based coordinate system. J. Cogn. Neurosci. 8, 1–28.

Drury, H.A., Van Essen, D.C., Corbetta, M., Snyder, A.Z., 1999. Surface-based analyses of the human cerebral cortex. In: Toga, A., et al. (Eds.), Brain Warping. Academic Press, New York, pp. 337–363.

Evans, A.C., Collins, D.I., Neelin, P., 1994. Three-dimensional correlative imaging: applications in human brain mapping. In: Thatcher, R.W., Hallett, M., Zeffiro, T., et al. (Eds.), Functional Neuroimaging: Technical Foundations. Academic Press, New York, pp. 145–162.

Fischl, B., Sereno, M.I., Dale, A.M., 1999a. Cortical surface-based analysis. II: Inflation, flattening, and a surface-based coordinate system. NeuroImage 9, 195–207.

Fischl, B., Sereno, M.I., Tootell, R.B., Dale, A.M., 1999b. High-resolution intersubject averaging and a coordinate system for the cortical surface. Hum. Brain Mapp. 8 (4), 272–284.

Friston, K.J., Holmes, A.P., Worsley, K.J., Poline, J.P., Frith, C.D., Frackowiak, R.S.J., 1995. Statistical parametric maps in functional imaging: a general linear approach. Hum. Brain Mapp. 2, 189–210.

Geyer, S., Schleicher, A., Zilles, K., 1999. Areas 3a, 3b and 1 of human primary somatosensory cortex. NeuroImage 10, 63–83.

Glaunes, J., Vaillant, M., Miller, M.I., 2004. Landmark matching via large deformation diffeomorphisms on the sphere. J. Math. Imaging Vis. 20, 179–200.

Grefkes, C., Geyer, S., Schormann, T., Roland, P., Zilles, K., 2001. Human somatosensory area 2: Observer-independent cytoarchitectonic mapping, individual variability, and population map. NeuroImage 14, 617–631.

Gu, X., Yau, S., 2002. Computing conformal structures of surfaces. Commun. Inform. Syst. 2, 121–146.

Holmes, C.J., Hoge, R., Collins, L., Woods, R., Toga, A.W., Evans, A.C., 1998. Enhancement of MR images using registration for signal averaging. J. Comput. Assist. Omag. 22, 324–333.

Jones, E.G., Peters, A., 1990a. Comparative structure and evolution of cerebral cortex. Part I. Cereb. Cortex vol. 8A. Kluwer Press, Boston.

Jones, E.G., Peters, A., 1990b. Comparative structure and evolution of cerebral cortex. Part II. Cereb. Cortex vol. 8A. Kluwer Press, Boston.

Joshi, S.C., Miller, M.I., Grenander, U., 1997. On the geometry and shape of brain sub-manifolds. Processing of MR Images of the Human Brain, Spec. Issue Int. J. Pattern Recogn. Artif. Intell. vol. 8, pp. 1317–1343.

Ju, L., Stern, J., Rhem, K., Schaper, K., Rottenberg, D.A., Hurdal, M.K., 2004. Cortical surface flattening using least square coformal mapping with minimal metric distortion. Proc. IEEE Int. Symp. Biomed. Imag., 77–80.

Kuperberg, G.R., Broome, M.R., McGuire, P.K., David, A.S., Eddy, M., Ozawa, F., Goff, D., West, W.C., Williams, S.C., van der Kouwe, A.J., Salat, D.H., Dale, A.M., Fischl, B., 2003. Regionally localized thinning of the cerebral cortex in schizophrenia. Arch. Gen. Psychiatry 60, 878–888.

Lewis, J.W., Van Essen, D.C., 2000. Mapping of architectonic subdivisions in the macaque monkey, with emphasis on parieto-occipital cortex. J. Comp. Neurol. 428, 79–111.

Ojemann, J.G., Akbudak, E., Snyder, A.Z., Mckinstry, R.C., Raichle, M.E., Conturo, T.E., 1997. Anatomic localization and quantitative analysis of gradient refocused echo-planar fMRI susceptibility artifacts. NeuroImage 6, 156–167.

Ono, M., Kubick, S., Abernathey, C.D., 1990. Atlas of the Cerebral Sulci. Thieme Medical, New York.

Orban, G.A., Van Essen, D., Vanduffel, W., 2004. Comparative mapping of higher visual areas in monkeys and humans. Trends Cogn. Sci. 8, 315–324.

Rademacher, J., Morosan, P., Schormann, T., Schleicher, A., Werner, C., Freund, H.-J., Zilles, K., 2001. Probabilistic mapping and volume measurement of human primary auditory cortex. NeuroImage 13, 669–683.

Rosas, H.D., Liu, A.K., Hersch, S., Glessner, M., Ferrante, R.J., Salat, D.H., van der Kouwe, A., Jenkins, B.G., Dale, A.M., Fischl, B., 2002. Regional and progressive thinning of the cortical ribbon in Huntington's disease. Neurology 58, 695–701.

Schwartz, E.L., Shaw, A., Wolfson, E., 1989. A numerical solution to the generalized mapmaker's problem: flattening nonconvex polyhedral surfaces. IEEE Trans. Pattern Anal. Mach. Intell. 11, 1005–1008.

Simon, O., Mangin, J.F., Cohen, L., LeBihan, D., Dehaene, S., 2002. Topographical layout of hand, eye, calculation, and language-related areas in the human parietal lobe. Neuron 33, 475–487.

Talairach, J., Tournoux, P., 1988. Coplanar Stereotaxic Atlas of the Human Brain. Thieme Medical, New York.

Thompson, P.M., Toga, A.W., 2002. A framework for computational anatomy. Comput. Vis. Sci. 5, 13–34.

Thompson, P.M., Woods, R.P., Mega, M.S., Toga, A.W., 2000. Mathematical/computational challenges in creating deformable and probabilistic atlases of the human brain. Hum. Brain Mapp. 9, 81–92.

Thompson, P.M., Hayashi, K.M., de Zubicaray, G., Janke, A.L., Rose, S.E., Semple, J., Herman, D., Hong, M.S., Dittmer, S.S., Doddrell, D.M., Toga, A.W., 2003. Dynamics of gray matter loss in Alzheimer's disease. J. Neurosci. 23, 994–1005.

Toga, A.W., 1999. Brain Warping. Academic Press, New York, pp. 385.

Ungerleider, L.G., Desimone, R., 1986. Cortical connections of visual area MT in the macaque. J. Comp. Neurol. 248, 190–222.

Van Essen, D.C., 1997. A tension-based theory of morphogenesis and compact wiring in the central nervous system. Nature 385, 313–318.

Van Essen, D.C., 2002. Windows on the brain. The emerging role of atlases and databases in neuroscience. Curr. Opin. Neurobiol. 12, 574–579.

Van Essen, D.C., 2004a. Organization of visual areas in Macaque and human cerebral cortex. In: Chalupa, L., Werner, J.S. (Eds.), The Visual Neurosciences. MIT Press, pp. 507–521.

Van Essen, D.C., 2004b. Surface-based comparisons of macaque and human cortical organization. In: Dehaene, S. (Ed.), From Monkey to Brain: Proceedings of a Fyssen Foundation Colloquium, June, 2003. MIT Press. In Press.

Van Essen, D.C., Newsome, W.T., Maunsell, J.H.R., 1984. The visual field representation in striate cortex of the macaque monkey: asymmetries, anisotropies and individual variability. Vis. Res. 24, 429–448.

Van Essen, D.C., Drury, H.A., Joshi, S., Miller, M.I., 1998. Functional and structural mapping of human cerebral cortex: solutions are in the surfaces. Proc. Natl. Acad. Sci. U. S. A. 95, 788–795.

Van Essen, D.C., Dickson, J., Harwell, J., Hanlon, D., Anderson, C.H., Drury, H.A., 2001. An integrated software system for surface-based analyses of cerebral cortex. J. Am. Med. Inform. Assoc. 8, 443–459.

Van Essen, D.C., Harwell, J., Hanlon, D., Dickson, J., 2004a. Surface-based atlases and a database of cortical structure and function. In: Koslow, S.H., Subramaniam, S. (Eds.), Databasing the Brain: From Data to Knowledge (Neuroinformatics). Wiley, New Jersey. In Press.

Van Essen, D.C., Snyder, A.Z., Raichle, M.E., Rose, F.E., Bellugi, U., 2004b. Differences in cortical shape in Williams Syndrome subjects compared to normal humans revealed by surface-based analysis. Soc. Neurosci. Abstr. (in press).

Van Horn, J.D., Grethe, J.S., Kostelec, P., Woodward, J.B., Aslam, J.A., Rus, D., Rockmore, D., Gazzaniga, M.S., 2001. The Functional Magnetic Resonance Imaging Data Center (fMRIDC): the challenges and rewards of large-scale databasing of neuroimaging studies. Philos. Trans. R. Soc. Lond., B Biol. Sci. 356, 1323–1339.

Wandell, B.A., Chial, S., Backus, B.T., 2000. Visualization and measurement of the cortical surface. J. Cogn. Neurosci. 12, 739–752.